

# Thermodynamic Properties of Adamantane Revisited

Ala B. Bazyleva,<sup>†</sup> Andrey V. Blokhin,<sup>†</sup> Gennady J. Kabo,<sup>\*,†</sup> Mikhail B. Charapennikau,<sup>†</sup> Vladimir N. Emel'yanenko,<sup>‡</sup> Sergey P. Verevkin,<sup>\*,‡</sup> and Vladimir Diky<sup>§</sup>

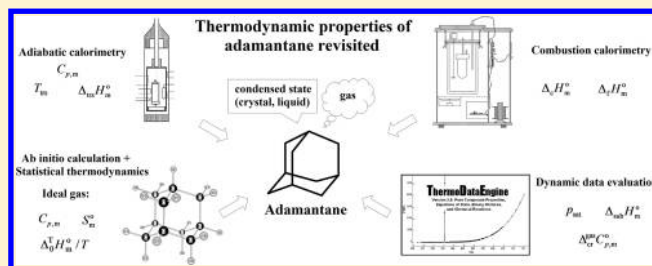
<sup>†</sup>Chemistry Faculty, Belarusian State University, Leningradskaya 14, 220030 Minsk, Belarus

<sup>‡</sup>Department of Physical Chemistry, University of Rostock, Dr-Lorenz-Weg-1, 18059 Rostock, Germany

<sup>§</sup>Thermophysical Properties Division, National Institute of Standards and Technology, 325 Broadway, Boulder, Colorado 80305-3337, United States

**S** Supporting Information

**ABSTRACT:** The heat capacity and parameters of the solid-to-solid phase transition of adamantane were measured in the temperature range from 80 to 370 K by use of adiabatic calorimetry. The thermodynamic functions for the compound in the crystalline and liquid states were calculated. The standard molar enthalpy of formation in the crystalline state for adamantane was obtained from combustion calorimetry by use of two different calorimeters. Available data on the enthalpy of combustion, saturated vapor pressure, and enthalpy of sublimation of adamantane were collected, analyzed, and selected. On the basis of spectroscopic data and results of quantum-chemical calculations, the ideal-gas properties for adamantane were calculated by a statistical thermodynamics method.



## 1. INTRODUCTION

The chemistry of adamantane has been attracting the attention of the scientific community for a long period of time. Surprisingly, thermodynamic properties for adamantane are scarce in the literature and are often not well established. However, these data are often used as key values for testing prediction methods and for reaction equilibrium calculations.<sup>1,2</sup> Heat capacities of adamantane in the temperature range from 5 to 350 K were measured by Chang and Westrum in 1960.<sup>3</sup> Determination of the heat capacity for the compound at higher temperatures to 600 K was performed in our laboratory in 2000.<sup>4</sup> A new attempt to determine the heat capacity in the low-temperature interval from 6 to 330 K was undertaken by van Ekeren et al.<sup>5</sup> in 2006, but they used a commercial sample without additional purification for the purpose of obtaining thermodynamic values of the solid-to-solid phase transition for adamantane as a calibration compound for routine DSC experiments. The heat capacity was presented in ref 5 only graphically and showed good agreement with the previous data<sup>3</sup> except for at temperatures greater than 270 K. In that region, the heat capacity of the commercial (not purified) sample of adamantane is linear but that of the highly pure sample by Chang and Westrum<sup>3</sup> shows a small broad hump. Unfortunately, van Ekeren et al.<sup>5</sup> did not discuss this discrepancy. In this context, new measurements of the heat capacity of carefully purified adamantane are necessary to determine if this anomaly really exists. The experimental data for the enthalpy of formation of adamantane are much more ambiguous. The scatter of 9 kJ·mol<sup>-1</sup> in the values available from the literature<sup>6–10</sup> is unacceptably large for this key property,

and new reliable measurements are required. Sublimation and vaporization enthalpies reported in refs 4, 6, and 8–20 and vapor pressures reported in refs 4, 8, 11, 13, 15, 16, and 18–20 also require critical evaluation because of significant discrepancies (up to 10 kJ·mol<sup>-1</sup> in  $\Delta_{\text{sub(vap)}}H_m^\circ$  and up to 30% in  $p_{\text{sat}}$ ).

In the present work, we report results of a comprehensive study of the heat capacity in the temperature range from 80 to 370 K and the combustion enthalpy of adamantane, the latter being measured in two laboratories independently. We also performed calculations of the thermodynamic functions in the condensed state from the heat-capacity data and those in the ideal-gas state by statistical thermodynamics by use of available spectroscopic data and results of quantum-chemical calculations. Evaporation parameters (sublimation enthalpy, vapor pressure) were critically evaluated by use of the ThermoData Engine software<sup>21–24</sup> with the enforcement of thermodynamic consistency between related properties based on published experimental data. The results of this work have allowed selection of the most reliable thermodynamic data for adamantane.

## 2. EXPERIMENTAL METHODS

**2.1. Sample Preparation.** *Sample 1 (Minsk).* Adamantane (Aldrich, initial mass-fraction purity > 0.99) was purified by triple recrystallization from acetone and subsequent sublimation at  $T = 333$  K under reduced pressure (the residual pressure of the pump

**Received:** May 23, 2011

**Revised:** July 13, 2011

**Published:** August 02, 2011

was 0.4 kPa). The sample was additionally sublimed in vacuum (the same pump) at the lower temperature,  $T = 307$  K, to remove any traces of moisture, and it was kept over  $P_2O_5$  for at least 1 week before measurements. The mass-fraction purity of this sample was 0.9980, as determined by GLC (Shimadzu GC-17A; stationary phase, RTX-1; column length, 30 m; carrier gas, nitrogen; flame-ionization detector). Only one minor impurity with a retention time very close to the main peak was detected. We assumed that this impurity was structurally similar to adamantane, and its contribution to uncertainties of the heat capacity or combustion energy is significantly smaller than other contributions, as discussed below.

**Sample 2 (Rostock).** A commercial sample of adamantane (Acros Organics; initial mass-fraction purity > 0.99) was purified by fractional vacuum sublimation at  $T = 353$  K. The final mass-fraction purity of adamantane, determined by GLC (Hewlett-Packard gas chromatograph 5890 Series II with a Hewlett-Packard 3390A integrator; stationary phase, cross-linked 5% PH ME silicone; column length, 25 m; carrier gas, nitrogen; flame-ionization detector) was 0.999. Sample 2 was also kept in a desiccator over  $P_2O_5$  before calorimetric measurements.

**2.2. Adiabatic Calorimetry.** Heat capacities at vapor saturation pressure for crystalline adamantane in the temperature range from 78 to 370 K and the temperature and enthalpy of its solid-phase (ordered crystal to plastic crystal) transition were measured in an automatic vacuum adiabatic calorimeter TAU-10 (Termis, Moscow, Russia) located in Minsk. The calorimeter, its testing, and uncertainty assessment were described in detail earlier.<sup>25</sup> The relative uncertainty of the  $C_{s,m}$  measurements was  $0.004C_{s,m}$  over the entire temperature range studied.<sup>25</sup> The repeatability of the heat-capacity measurements was better than 0.1% of the measured value.

A titanium calorimetric cell ( $V \approx 1.0$  cm<sup>3</sup>) was loaded with solid adamantane (Sample 1) of 0.6855 g and then degassed in vacuum with a residual pressure of  $\approx 3$  Pa over a 0.5 h period. Helium (at  $p \approx 5$  kPa and  $T = 290$  K) was introduced into the internal free space of the cell to facilitate heat transfer during the measurements. The container was sealed by use of an indium ring and a titanium head fixed with a copper screw. The heat-capacity ratio  $c_s(\text{sample})/\{c_s(\text{sample}) + c_s(\text{cell})\}$  was about 0.3–0.4.

An iron–rhodium resistance thermometer (ITS-90;  $R_0 = 50$   $\Omega$ ; calibrated by VNIIFTRI, Moscow, Russia) placed on the inner surface of the adiabatic shield was used for the temperature measurements in the calorimetric experiments. The temperature difference between the shield and the cell was determined by a differential (copper + 0.001 iron)/Chromel thermocouple. Adiabatic conditions were maintained to  $\pm 10^{-3}$  K.

Heating periods in the calorimetric experiments were 400 s; the period of thermal relaxation was approximately 150 s, except in the phase-transition region, where this period could be automatically prolonged. The periods of temperature-drift measurements were set to 400 s in most series and to 1500–1600 s in some series in the vicinity of the phase transition (Series 4 and 5). The temperature step was about 1.6 to 2.1 K in the “normal” heat-capacity measurements and did not exceed 0.10 K during the measurements of the triple point.

The corrections for adjustment of  $C_{s,m}$  to  $C_{p,m}$  and for sublimation of adamantane into the free space of the calorimetric cell were negligible. Their total contribution was less than  $10^{-3}$   $C_{s,m}$  near 370 K and therefore was not taken into consideration.

The temperature corresponding to the cusp points on the  $C_{s,m}$  against  $T$  curve and determined in independent measurements

with a temperature step of not more than 0.1 K was assumed to be the temperature of the solid-to-solid transition ( $T_{\text{trs}}$ ). The transition enthalpy was determined by averaging the results of single-step experiments. The initial ( $T_{\text{start}}$ ) and final ( $T_{\text{end}}$ ) temperatures of these experiments lay outside the phase-transition region. The  $\Delta_{\text{trs}}H_m^o$  value was calculated according to

$$\Delta_{\text{trs}}H_m^o = Q - \int_{T_{\text{start}}}^{T_{\text{trs}}} C_{p,m}(\text{crII})dT - \int_{T_{\text{trs}}}^{T_{\text{end}}} C_{p,m}(\text{crI})dT \quad (1)$$

where  $Q$  is the energy required for heating 1 mol of the compound from  $T_{\text{start}}$  to  $T_{\text{end}}$  and  $C_{p,m}(\text{crII})$  and  $C_{p,m}(\text{crI})$  are the normal molar heat capacities of the low- and high-temperature phases in the phase-transition region, respectively.

**2.3. Bomb Combustion Calorimetry.** The enthalpy of combustion of crystalline adamantane was measured by use of two different calorimeters. We used a semiautomatic combustion calorimeter with an isothermal air bath and a static bomb, which was designed and constructed in our laboratory in Minsk. A static-bomb isoperibol calorimeter with a stirred water bath (a redesigned commercial V-08-MA calorimeter) was used in Rostock.

**2.3.1. Air-Bath Calorimeter (Minsk).** The design of the calorimeter and the measurement procedure have been described in detail earlier.<sup>26</sup> The temperature of the bath was maintained at  $T_{\text{bath}} = 301.65 \pm 0.02$  K. The volume of the bomb was 95.6 cm<sup>3</sup>. The calibration of the calorimeter was carried out by use of reference benzoic acid (K-3 grade, mass-fraction purity of 0.99992, VNIIM, Russia) having a certified value of the combustion energy under the bomb conditions  $-26\,434 \pm 5$  J  $\cdot$  g<sup>-1</sup>. The energy equivalent of the bomb calorimeter is  $\epsilon_{\text{calor}} = 9826.0 \pm 2.5$  J  $\cdot$  K<sup>-1</sup> (from 19 calibration experiments, twice the standard deviation of the mean is given). Sample 1 was used. Weighing was carried out on a Mettler Toledo AG 245 electronic balance with a repeatability of  $\pm 2 \times 10^{-5}$  g (device specification). Since adamantane is a volatile compound, the samples were pressed into pellets and burned in hermetically sealed terylene bags. The standard state combustion energy for terylene determined in an independent series of experiments is  $\Delta_c u^o(298.15 \text{ K}) = -22\,803 \pm 35$  J  $\cdot$  g<sup>-1</sup> (twice the standard deviation of the mean).<sup>26</sup> The encapsulated samples were suspended on a platinum wire (0.05 mm diameter) used for ignition and burned in oxygen. The bomb was flushed with oxygen three times before final charging. The exact value of pressure in each experiment was obtained from the difference of the bomb masses after and before charging with oxygen (weighing repeatability of  $\pm 0.02$  g). The oxidation of nitrogen (an impurity in oxygen) was taken into account: 1.00 cm<sup>3</sup> of water was introduced into the bomb before an experiment; after combustion, wash water from the bomb was titrated with 0.1 mol  $\cdot$  dm<sup>-3</sup> NaOH aqueous solution. The combustion products were examined for traces of soot. Its quantity did not exceed 0.10 mg, determined from the masses of the crucible dried in air after an experiment and after removal of the soot formed. The contribution of incomplete burning was calculated with the use of the average combustion energy for soot,  $\Delta_c u^o(298.15 \text{ K}) = -33$  kJ  $\cdot$  g<sup>-1</sup>, according to the method described in ref 27. In a previous paper,<sup>26</sup> it was shown that formation of soot (not more than 0.2 mg) is not accompanied by any noticeable amount of CO (the energy input from oxidation of CO traces to CO<sub>2</sub> is less than 0.006% of the total energy released in the bomb).

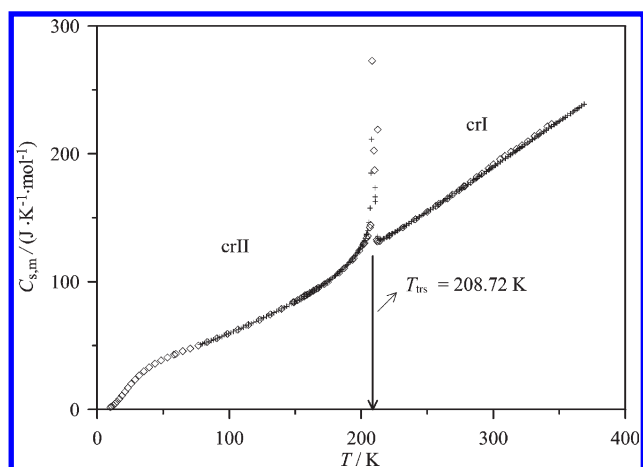


**Figure 1.** Temperature dependence of the molar heat capacity of adamantane in the crystalline state: (+) results obtained in this work; (◇) data by Chang and Westrum.<sup>3</sup>

**2.3.2. Water-Bath Calorimeter (Rostock).** The detailed experimental procedure has been described previously.<sup>28</sup> The water bath temperature was  $T_{\text{bath}} = 300.65 \pm 0.01$  K. The volume of the bomb was  $320 \text{ cm}^3$ . The energy equivalent of the calorimeter,  $\varepsilon_{\text{calor}} = 14\,810.5 \pm 1.5 \text{ J} \cdot \text{K}^{-1}$  (twice the standard deviation of the mean), was determined in a series of 11 experiments with a standard reference sample of benzoic acid (sample SRM 39j, NIST, USA). In this study, we used commercially available  $1 \text{ cm}^3$  polyethylene bulbs (Fa. NeoLab, Heidelberg, Germany) as sample containers for adamantane to avoid evaporation. The standard state combustion energy for the polyethylene used was measured to be  $\Delta_{\text{c}}u^\circ(298.15 \text{ K}) = -46\,352.1 \pm 7.0 \text{ J} \cdot \text{g}^{-1}$  (twice the standard deviation of the mean). Sample 2 was used. Weighing using a Mettler electronic balance was carried out with a repeatability of  $\pm 2 \times 10^{-6} \text{ g}$  (device specification). The combustion was performed in an oxygen atmosphere at  $p = 3.04 \text{ MPa}$ , without flushing before charging the bomb. A cotton thread was used as a fuse, whose combustion energy was determined in this work:  $\Delta_{\text{c}}u^\circ(298.15 \text{ K}) = -16\,945.2 \pm 8.4 \text{ J} \cdot \text{g}^{-1}$  (twice the standard deviation of the mean). Correction for nitric acid formation was based on titration with  $0.1 \text{ mol} \cdot \text{dm}^{-3} \text{ NaOH (aq)}$ . The combustion products were examined for the absence of carbon monoxide (Dräger tube). In contrast to the experiments in Minsk, unburned carbon (soot) was not detected in the combustion experiments.

Treatment of the results obtained with both calorimeters was carried out in accordance with recommended calculation procedures.<sup>27,29</sup> The sample masses were reduced to vacuum conditions taking into consideration the density values given in Table S1 (Supporting Information). For converting the energy of the actual bomb process to that of an isothermal process and reducing to the standard state (Washburn's corrections), the conventional procedure<sup>29</sup> was applied with the use of the data from Table S1 (Supporting Information). The atomic masses used were those from the IUPAC Technical Report:<sup>30</sup> as adamantane is obtained from oil sources, the average relative atomic masses of carbon and hydrogen ( $12.0108 \pm 0.0002$  and  $1.00796 \pm 0.00001$ ) were accepted in accordance with Figures 2 and 3 of ref 30.

### 3. RESULTS AND DISCUSSION

**3.1. Heat Capacity and Phase-Transition Parameters in the Condensed State.** Experimental values of the molar heat

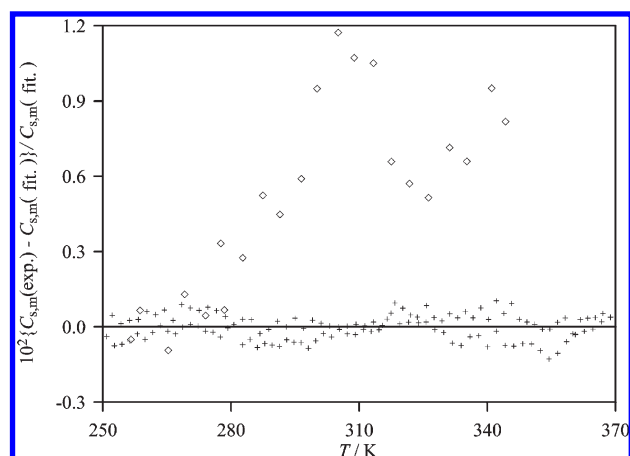


**Figure 2.** Deviation of the experimental heat capacities of adamantane from the fitting curve: (+) results obtained in this work; (◇) data by Chang and Westrum.<sup>3</sup>

**Table 1.** Enthalpy of the Solid-to-Solid Phase Transition (crII  $\rightarrow$  crI) for Adamantane<sup>a</sup>

$T_{\text{start}}$ (K)	$T_{\text{end}}$ (K)	$Q$ ( $\text{J} \cdot \text{mol}^{-1}$ )	$\Delta_{\text{trs}}H_{\text{m}}^\circ$ ( $\text{J} \cdot \text{mol}^{-1}$ )
169.31	217.82	8782	3286
168.93	217.81	8809	3278
168.56	216.63	8676	3268
169.08	215.02	8419	3274

$$\Delta_{\text{trs}}H_{\text{m}}^\circ = (3276 \pm 12)^b$$

<sup>a</sup>The heat-capacity baselines for crII and crI used for the calculation of  $\Delta_{\text{trs}}H_{\text{m}}^\circ$  are eqs 2 and 3, respectively. <sup>b</sup>The average value.

capacity  $C_{\text{s,m}}$  of adamantane in the temperature range from 78 to 370 K are presented in Table S2 (Supporting Information) and Figure 1, where a comparison with the heat-capacity results by Chang and Westrum<sup>3</sup> (adjusted to ITS-90) is also given.

Our  $C_{\text{s,m}}$  values agree well with those from ref 3 within  $\pm(0.2\text{--}0.4\%)$  at  $T < 270$  K. However, at higher temperatures, the heat capacity obtained by us behaves linearly whereas that of Chang and Westrum<sup>3</sup> shows irregularity and becomes larger than ours up to 1.2% (Figure 2). The same problem with the heat capacity from ref 3 was observed by van Ekeren et al.<sup>5</sup> as mentioned in the Introduction. The differences observed could be due to water traces in the sample or some technical reasons (temperature scale shift, insufficient sealing of the cell, lack of adiabatic conditions at high temperature, etc.). Thus, we considered the data below 270 K from ref 3 as reliable and used them together with our own to evaluate the transition enthalpy and the derived thermodynamic functions. The heat capacities above 270 K from ref 3 were rejected.

As mentioned above, the high-temperature determination of heat capacity of adamantane between 340 and 600 K was performed by differential scanning calorimetry in our laboratory earlier.<sup>4</sup> The data of adiabatic calorimetry and DSC agree within 2%, which corresponds to the uncertainty of the DSC results. Hence, the results from the previous paper<sup>4</sup> were also used to derive thermodynamic functions of adamantane at temperatures above 370 K but with a smaller weighting factor (based on the

Table 2. Standard Molar Thermodynamic Functions of Adamantane in the Crystalline and Liquid States

$T$ (K)	$C_{p,m}^{\circ}$ ( $J \cdot K^{-1} \cdot mol^{-1}$ )	$\Delta_0^T H_m^{\circ}/T$ ( $J \cdot K^{-1} \cdot mol^{-1}$ )	$\Delta_0^T S_m^{\circ}$ ( $J \cdot K^{-1} \cdot mol^{-1}$ )	$\Phi_m^{\circ}$ ( $J \cdot K^{-1} \cdot mol^{-1}$ )
crystal II				
5	0.1545	0.0386	0.0515	0.0129
10	1.642	0.3533	0.4598	0.1064
15	6.131	1.451	1.877	0.4262
20	12.56	3.407	4.501	1.094
25	19.08	5.898	8.013	2.115
30	24.82	8.587	12.01	3.427
35	29.58	11.26	16.21	4.953
40	33.44	13.80	20.42	6.624
45	36.60	16.16	24.55	8.387
50	39.23	18.34	28.54	10.20
60	43.67	22.20	36.10	13.90
70	47.58	25.55	43.13	17.58
80	51.39	28.54	49.73	21.19
90	55.38	31.30	56.01	24.71
100	59.65	33.92	62.06	28.14
110	64.12	36.46	67.96	31.50
120	68.81	38.96	73.73	34.78
130	73.76	41.44	79.44	37.99
140	78.96	43.94	85.09	41.15
150	84.45	46.45	90.72	44.27
160	90.24	49.01	96.36	47.35
170	96.35	51.61	102.0	50.40
180	102.8	54.27	107.7	53.42
190	109.6	57.00	113.4	56.43
200	116.8	59.81	119.2	59.43
208.72	123.3	62.33	124.4	62.03
crystal I				
208.72	128.5	78.02	140.1	62.03
210	129.3	78.33	140.8	62.51
220	135.3	80.79	147.0	66.21
230	141.6	83.29	153.2	69.86
240	148.1	85.86	159.3	73.46
250	154.7	88.48	165.5	77.01
260	161.6	91.16	171.7	80.54
270	168.6	93.90	177.9	84.03
280	175.7	96.69	184.2	87.49
290	182.8	99.54	190.5	90.94
298.15	188.6	101.9	195.6	93.73
300	189.9	102.4	196.8	94.36
310	197.1	105.4	203.1	97.76
320	204.3	108.3	209.5	101.2
330	211.5	111.4	215.9	104.5
340	218.6	114.4	222.3	107.9
350	225.6	117.5	228.8	111.3
360	232.7	120.6	235.2	114.6
370	239.8	123.7	241.7	118.0
380	247	127	248	121
390	254	130	255	125
400	262	133	261	128
410	269	136	268	131
420	277	140	274	135



Table 2. Continued

$T$ (K)	$C_{p,m}^{\circ}$ ( $J \cdot K^{-1} \cdot mol^{-1}$ )	$\Delta_0^T H_m^{\circ}/T$ ( $J \cdot K^{-1} \cdot mol^{-1}$ )	$\Delta_0^T S_m^{\circ}$ ( $J \cdot K^{-1} \cdot mol^{-1}$ )	$\Phi_m^{\circ}$ ( $J \cdot K^{-1} \cdot mol^{-1}$ )
430	284	143	281	138
440	292	146	288	141
450	299	150	294	145
460	307	153	301	148
470	315	156	308	151
480	322	160	314	155
490	330	163	321	158
500	337	166	328	161
510	345	170	334	165
520	352	173	341	168
530	360	177	348	171
540	367	180	355	175
543.2	370	181	357	176
liquid				
543.2	370	207	383	176
550	375	209	387	178
560	382	212	394	182
570	389	215	401	186
580	396	218	408	190
590	402	221	415	193
600	409	224	421	197

relative uncertainty of the methods) than that for the results from adiabatic calorimetry.

One solid-to-solid transition was found in the studied temperature interval. It is associated with formation of orientationally disordered (plastic) crystals. The transition temperature is determined to be  $T_{\text{trs}} = 208.72 \pm 0.05$  K. Chang and Westrum<sup>3</sup> reported  $T_{\text{trs}} = 208.67$  K (adjusted to the ITS-90) for this phase transition, in excellent agreement with our value.

The enthalpy and entropy of the  $\text{crII} \rightarrow \text{crI}$  transition,  $\Delta_{\text{trs}} H_m^{\circ} = 3276 \pm 12$   $J \cdot mol^{-1}$  and  $\Delta_{\text{trs}} S_m^{\circ} = 15.70 \pm 0.06$   $J \cdot K^{-1} \cdot mol^{-1}$ , were obtained by averaging the results of the single-step experiments in the adiabatic calorimeter (Table 1). The heat capacities of the phases  $\text{crII}$  and  $\text{crI}$

$$C_{p,m}(\text{crII})/(J \cdot K^{-1} \cdot mol^{-1}) = 23.55 + 0.3165(T/K) + 1.436 \times 10^{-4}(T/K)^2 + 3.022 \times 10^{-6}(T/K)^3 \quad (2)$$

$$C_{p,m}(\text{crI})/(J \cdot K^{-1} \cdot mol^{-1}) = 50.80 + 0.1527(T/K) + 1.052 \times 10^{-3}(T/K)^2 \quad (3)$$

were obtained from the experimental values from  $T = 83$  to  $155$  K and from  $214$  to  $269$  K for  $\text{crII}$  and  $\text{crI}$ , respectively.

Chang and Westrum<sup>3</sup> obtained the transition enthalpy to be  $3376 \pm 4$   $J \cdot mol^{-1}$ . The deviation between the  $\Delta_{\text{trs}} H_m^{\circ}$  values reported by Chang and Westrum<sup>3</sup> and from our measurements arises from the subjective choice of heat-capacity baselines in the transition range. In this work, two independent baselines for the low- and high-temperature crystals were chosen, whereas Chang and Westrum<sup>3</sup> used a common baseline for both phases. However, the latter choice does not seem reasonable since the transition is apparently first order (as noted in ref 3), but this

choice made it of  $\lambda$  type in a wide temperature range. Thus, only the value for the transition enthalpy obtained in the present work was further applied. The only value that does not depend on any ambiguity and can be compared is the energy input necessary to heat the compound from a temperature well below the transition to a temperature well above it. The values of  $\Delta_{150}^{250} H_m^{\circ}$  are  $15\,167 \pm 15$   $J \cdot mol^{-1}$  from ref 3 and  $15\,152 \pm 61$   $J \cdot mol^{-1}$  from the present measurements, and are in excellent agreement.

Extrapolation of the heat capacity to  $T = 0$  K for phase  $\text{crII}$  from ref 3 was carried out with a Debye function with three degrees of freedom:  $C_{p,m} = 3R \cdot D(\langle \Theta_D \rangle / T)$ . The average Debye characteristic temperature  $\langle \Theta_D \rangle = 116.3 \pm 1.5$  K was determined from the experimental heat capacities within  $5.1$  to  $6.8$  K, i.e., from the lowest measured temperature to the temperature above which the Debye model failed to describe the observed temperature dependence of  $C_{p,m}$ .

The thermodynamic properties of adamantane in the condensed state between  $T = 5$  and  $600$  K (Table 2) were derived on the basis of the smoothed heat capacity and the parameters of its phase transitions. The fusion parameters from ref 4 ( $T_{\text{fus}} = 543.2$  K and  $\Delta_{\text{fus}} H_m^{\circ} = 13.96 \pm 0.28$   $kJ \cdot mol^{-1}$ ) were accepted.

**3.2. Thermodynamic Functions in the Ideal-Gas State.** The procedure for statistical thermodynamics calculations of ideal gases is presented in detail in ref 31. It was estimated that the error of the calculations by statistical thermodynamics did not exceed  $\pm 0.5\%$ .

The molar mass of adamantane is  $M = 0.136235$   $kg \cdot mol^{-1}$ , and the symmetry of its overall rotation is  $T_d$  (symmetry number  $\sigma = 12$ ). The molecular geometry of adamantane was found by optimization in the PC GAMESS software (version 7.0)<sup>32</sup> at the B3LYP/6-311G\* theory level. Thus, the product of the main inertia moments was derived to be  $I_A \cdot I_B \cdot I_C = 1.2535 \times 10^{-133}$   $kg^3 \cdot m^6$ .

**Table 3.** Standard Molar Thermodynamic Functions of Adamantane in the Ideal Gaseous State ( $R = 8.314472 \text{ J} \cdot \text{K}^{-1} \cdot \text{mol}^{-1}$ ,  $p^\circ = 10^5 \text{ Pa}$ )

$T \text{ (K)}$	$C_{p,m}$ ( $\text{J} \cdot \text{K}^{-1} \cdot \text{mol}^{-1}$ )	$\Delta_0^T H_m^\circ / T$ ( $\text{J} \cdot \text{K}^{-1} \cdot \text{mol}^{-1}$ )	$\Delta_0^T S_m^\circ$ ( $\text{J} \cdot \text{K}^{-1} \cdot \text{mol}^{-1}$ )	$\Phi_m^\circ$ ( $\text{J} \cdot \text{K}^{-1} \cdot \text{mol}^{-1}$ )	$\Delta_f H_m^\circ$ ( $\text{kJ} \cdot \text{mol}^{-1}$ )	$\Delta_f G_m^\circ$ ( $\text{kJ} \cdot \text{mol}^{-1}$ )
0	0	0	0	0	−75.2	−75.2
50	33.52	33.29	209.9	176.6	−84.5	−63.8
100	42.54	35.06	235.0	200.0	−96.3	−38.2
150	61.69	40.58	255.7	215.1	−105.7	−7.2
200	86.22	48.81	276.7	227.9	−114.8	27.1
298.15	147.8	70.88	322.1	251.2	−132.3	100.5
300	149.1	71.36	323.0	251.7	−132.6	101.9
400	216.9	99.34	375.3	276.0	−147.8	182.5
500	277.1	129.0	430.4	301.3	−159.6	266.5
600	327.1	158.0	485.4	327.4	−168.5	352.6
700	368.3	185.2	539.1	353.9	−174.9	440.0
800	402.5	210.3	590.5	380.2	−179.2	528.6
900	431.2	233.3	639.6	406.4	−181.6	616.7
1000	455.4	254.3	686.4	432.0	−182.5	705.5
1100	476.0	273.6	730.8	457.2	−182.2	794.3
1200	493.6	291.2	772.9	481.8	−180.8	883.0
1300	508.6	307.3	813.1	505.7	−178.6	971.6
1400	521.5	322.2	851.2	529.0	−175.8	1060
1500	532.7	335.9	887.6	551.7	−172.5	1048

Experimental vibrational IR and Raman spectra for adamantane (crystal or solutions in  $\text{C}_6\text{H}_6$  and  $\text{CS}_2$ ) were taken from the literature.<sup>33–35</sup> No significant shifts (more than  $5 \text{ cm}^{-1}$ ) between the vibrational spectra for the crystalline phase and those in solution were observed. Since adamantane is a highly symmetrical molecule, there are a number of vibrations that are not observed in both spectra and cannot be determined experimentally. In order to complete the set of wave numbers describing the normal vibrations necessary for the statistical thermodynamics calculations, we also used the fundamentals calculated by QCISD/6-311G\*, B3LYPultrafine/6-31G\*, CCD/6-311G\*, and MP2-(full)/6-311G\* from ref 36. The wave numbers calculated by the ab initio methods were scaled using factors (Table S3, Supporting Information) obtained in this work after the calculated fundamentals had been assigned to the corresponding experimental ones. The average and maximum deviations between calculated (scaled) and experimental fundamentals (excluding the hardly analyzable region from 2800 to  $3000 \text{ cm}^{-1}$  corresponding to the C–H stretching vibrations) for adamantane amounted to 5 and  $9 \text{ cm}^{-1}$  for QCISD/6-311G\*, 6 and  $13 \text{ cm}^{-1}$  for B3LYPultrafine/6-31G\*, 5 and  $9 \text{ cm}^{-1}$  for CCD/6-311G\*, and 7 and  $14 \text{ cm}^{-1}$  for MP2(full)/6-311G\*, respectively. Thus, the following complete set of the wave numbers for the statistical thermodynamics calculations was compiled (the values in parentheses are corresponding degeneracies; the italic font identifies wave numbers taken from the quantum-chemical calculations): 2940 (3), 2915 (3), 2915, 2910 (3), 2900 (2), 2855, 2850 (3), 1472, 1451 (3), 1437 (2), 1371 (2), 1354 (3), 1321 (3), 1310 (3), 1288 (3), 1218 (2), 1106 (3), 1106, 1100 (3), 1044 (3), 1041, 970 (3), 911 (2), 885 (3), 801 (3), 757, 639 (3), 444 (3), 401 (2), 317 (3). The experimental fundamentals were used when available, with solution spectra being preferred.

The standard thermodynamic properties of adamantane in the ideal gaseous state from 0 to 1500 K are summarized in Table 3.

**3.3. Vapor Pressure and Evaporation Enthalpy.** The sublimation pressure and sublimation enthalpy for adamantane were evaluated with the NIST ThermoData Engine 103b software (Thermodynamics Research Center of the National Institute of Standards and Technology, Boulder, CO)<sup>21–24</sup> based on joint processing of vapor and sublimation pressures, heat capacity in the crystalline and gaseous phases, enthalpies of fusion and sublimation, and gas densities based on estimated virial coefficients. Experimental values of saturated vapor pressure for solid adamantane<sup>4,8,13,15,16,18–20</sup> and for liquid adamantane,<sup>11,13</sup> as well as of sublimation enthalpy<sup>4,9,10,14,17</sup> and vaporization enthalpy<sup>11,12</sup> were involved. Although the vapor and sublimation pressures reported in ref 13 are consistent with the enthalpy of fusion (at  $T_{\text{fus}} = 543.2 \text{ K}$ ) within the evaluated uncertainty, they proved to be inconsistent with the low-temperature sublimation data and their inclusion did not increase the accuracy or reliability of the evaluation (Figure 3). The vapor pressure and vaporization enthalpy at 298.15 K for liquid adamantane determined by gas chromatography<sup>11,12</sup> were not used in the data analysis because the hypothetical liquid state at 298.15 K is undercooled by 245 K below the fusion temperature 543.2 K and such a large extrapolation of the properties would be very unreliable.

The objective function for the joint processing of different property data was a sum of objective functions for equations describing separate properties and objective functions for the thermodynamic consistency constraints, as implemented in ThermoData Engine.<sup>21,22</sup> The consistency conditions included those between sublimation pressure and enthalpy of sublimation (taking into account the difference of compressibility factors of the condensed and gas phases), between enthalpy of sublimation and the difference of heat capacities of the condensed and gas phases, between liquid vapor and sublimation pressures at the triple point, and between enthalpies of vaporization (derived from vapor pressure), sublimation, and fusion at the triple point. After exclusion of vapor pressure data for the liquid, due to their

large uncertainty and disagreement with most other data, the last two conditions were dropped.

The joint processing of this data revealed the only reliable source of sublimation pressures, ref 15 (Figure 3). The resulting sublimation pressure equation between  $T = 254$  and  $543$  K over crI is the following

$$\ln(p/\text{kPa}) = 50.9129 - 8494.5 \cdot (T/\text{K})^{-1} - 4.6395 \cdot \ln(T/\text{K}) \quad (4)$$

which is in good agreement with the sublimation enthalpy data.<sup>4,9,10,17</sup> The authors of ref 14 mentioned that the sublimation enthalpy at  $T = 298.15$  K obtained in that work was less reliable because of a large temperature adjustment. Indeed, it showed a large deviation from the values derived from the sublimation pressure given by eq 4 (Figure 4) and, hence, was excluded from the joint data treatment.

The difference between heat capacities of gas and crystal can be expressed from eq 4 at  $p_{\text{sat}} \ll 1$  bar as

$$\Delta_{\text{cr}}^{\text{gas}} C_{p,m} = R \frac{d}{dT} \left[ \frac{d \ln p_{\text{sat}}}{d(1/T)} \right] \quad (5)$$

equal to  $-38.6 \text{ J} \cdot \text{K}^{-1} \cdot \text{mol}^{-1}$  at  $T = 298.15$  K. This agrees with the difference  $-40.8 \text{ J} \cdot \text{K}^{-1} \cdot \text{mol}^{-1}$  between the values  $147.8 \pm 0.7 \text{ J} \cdot \text{K}^{-1} \cdot \text{mol}^{-1}$  (gas, statistical thermodynamics, Table 3) and  $188.6 \pm 0.8 \text{ J} \cdot \text{K}^{-1} \cdot \text{mol}^{-1}$  (crystal, adiabatic calorimetry, Table 2) obtained in this work.

The following values can be derived by eq 4 at  $T = 298.15$  K: sublimation enthalpy  $\Delta_{\text{sub}} H_m^{\circ} = 59.13 \pm 0.91 \text{ kJ} \cdot \text{mol}^{-1}$  and sublimation pressure  $p_{\text{sat}} = 18.1 \pm 0.9 \text{ Pa}$ . These values together with the standard entropy of crystalline adamantane,  $\Delta_0^{\text{T}} S_m^{\circ}(\text{cr}) = 195.6 \pm 0.9 \text{ J} \cdot \text{K}^{-1} \cdot \text{mol}^{-1}$  (Table 2), were used for calculation of the standard entropy in the ideal gaseous state at  $T = 298.15$  K

$$\Delta_0^{\text{T}} S_{m,\text{exp}}^{\circ}(\text{g}, T) = \Delta_0^{\text{T}} S_m^{\circ}(\text{cr}, T) + \frac{\Delta_{\text{sub}} H_m^{\circ}(T)}{T} + R \ln \left( \frac{p_{\text{sat}}(T)}{p^{\circ}} \right) = (322.3 \pm 3.2) \text{ J} \cdot \text{K}^{-1} \cdot \text{mol}^{-1} \quad (6)$$

This value is in good agreement with the ideal-gas entropy  $322.1 \pm 1.6 \text{ J} \cdot \text{K}^{-1} \cdot \text{mol}^{-1}$  calculated by the statistical thermodynamics method (Table 3).

**3.4. Enthalpy of Combustion and Formation in the Crystalline State.** Results of the combustion experiments for adamantane using two types of calorimeter at  $T = 298.15$  K are summarized in Tables S4 and S5 (Supporting Information). Values of the molar standard energies of combustion  $\Delta_c U_m^{\circ}$ , together with their repeatability are also given in Tables S4 and S5 (Supporting Information) for each series separately. The resulting enthalpies of combustion,  $\Delta_c H_m^{\circ}$ ,  $-6030.2 \pm 2.7 \text{ kJ} \cdot \text{mol}^{-1}$  (Minsk) and  $-6032.2 \pm 2.9 \text{ kJ} \cdot \text{mol}^{-1}$  (Rostock) measured in this work by use of different calorimeters, different samples, and different purification procedures agree well. Our results are also in agreement with most other combustion results (Table 4), except for the result from ref 6. For the sake of uniformity, we recalculated the uncertainties reported in the original work,<sup>6–10</sup> as well as calculated the uncertainty for our results including repeatability (twice the overall standard deviation of the mean), calibration uncertainty, and uncertainty of the combustion energy of benzoic acid and auxiliary compounds. If

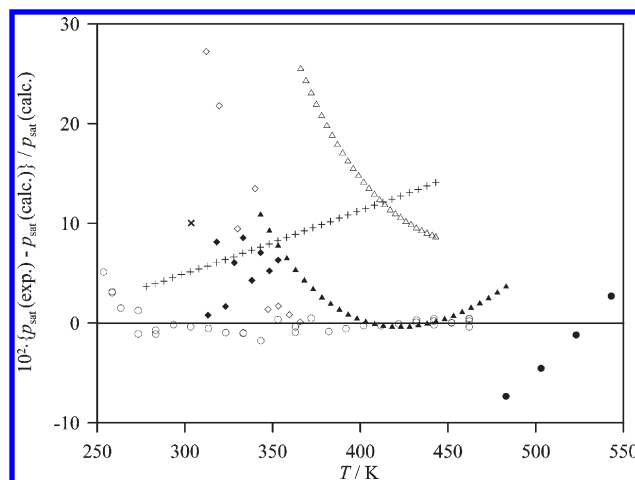


**Figure 3.** Relative deviations of sublimation pressure data from eq 4 for adamantane: (x) from ref 4; (Δ) from ref 8; (●) from ref 13; (○) from ref 15; (▲) from ref 16; (+) from ref 18; (◇) from ref 19; (◆) from ref 20.

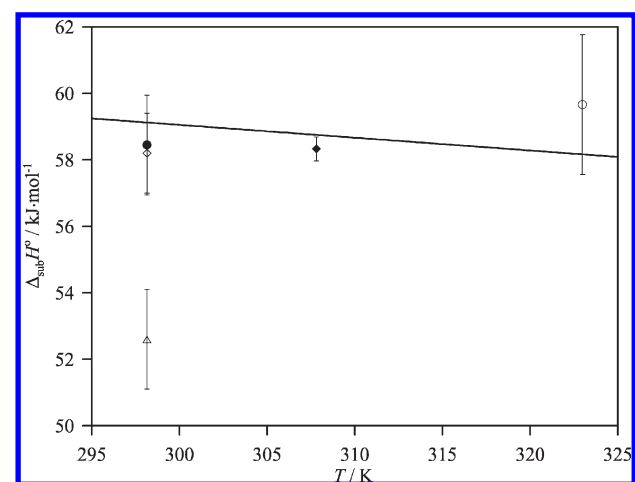


**Figure 4.** Sublimation enthalpy data for adamantane: (◆) from ref 4; (○) from ref 9; (◇) from ref 10; (Δ) from ref 14; (●) from ref 17; (—) from eq 4.

any uncertainty contribution was not presented in a reference, an estimate was made based on the previous work of the corresponding authors.

Unexpectedly, the largest deviation from the other  $\Delta_c H_m^{\circ}$  values (see Table 4) was found for that of Månsson et al.<sup>6</sup> measured in one of the most respected thermochemical laboratories of the time. As a possible explanation, we noticed that the same adamantane sample was used for combustion experiments<sup>6</sup> and heat capacity measurements,<sup>3</sup> where an anomaly at  $T > 270$  K was observed (see discussion in section 3.1). It is possible that water, occluded or adsorbed on the surface of the sample, could lead to such results. To check this hypothesis, several combustion experiments were performed with Sample 1 without drying for a week in a desiccator with  $\text{P}_2\text{O}_5$ . Values of  $\Delta_c U_m^{\circ}$  about  $7 \text{ kJ} \cdot \text{mol}^{-1}$  higher were obtained. This is consistent with water contamination, resulting in less energy released upon combustion. There is no information about drying of the sample in ref 6, and we conclude that this could be the source of the discrepancy.

We also carefully analyzed the primary data and experimental conditions reported in the original sources. In all cases, the vitally

Table 4. Enthalpy of Combustion and Formation of Adamantane in the Crystalline State at 298.15 K<sup>a</sup>

$\Delta_c H_m^\circ$ (kJ·mol <sup>-1</sup> )	$\Delta_f H_m^\circ$ (kJ·mol <sup>-1</sup> )	purity/purification method	auxiliary compounds	source
-6024.4 ± 0.7	-197.4 ± 1.5	<0.999/recryst.	cotton, mylar	<i>b</i>
-6033.2 ± 2.5	-188.5 ± 2.8	<0.9995/recryst., subl.	cotton, Melinex, hydrocarbon oil	<i>c</i>
-6033.0 ± 4.3	-188.7 ± 4.5	n.a./subl.	cotton, mylar	<i>d</i>
-6029.2 ± 1.5	-192.6 ± 2.0	<0.9999/n.a.	polyethylene, paper	<i>e</i>
-6028.3 ± 2.8	-193.4 ± 3.1	n.a./n.a.	n.a.	<i>f</i>
-6030.2 ± 2.7	-191.6 ± 3.0	<0.998/recryst., subl.	terylene	this work, Minsk
-6032.3 ± 2.9	-189.5 ± 3.2	<0.999/subl.	cotton, polyethylene	this work, Rostock

<sup>a</sup> Recalculated using the 2009 atomic masses of elements<sup>30</sup> and the formation enthalpies of gaseous CO<sub>2</sub>,  $\Delta_f H_m^\circ$  (CO<sub>2</sub>, g) = -393.51 ± 0.13 kJ·mol<sup>-1</sup>, and liquid H<sub>2</sub>O,  $\Delta_f H_m^\circ$  (H<sub>2</sub>O, liq) = -285.83 ± 0.04 kJ·mol<sup>-1</sup>.<sup>37</sup> The combined uncertainty is given; it was obtained from repeatability (twice the standard deviation of the mean), calibration uncertainty, uncertainty of combustion energy of benzoic acid and auxiliary compounds (if any uncertainty contribution was not presented in a reference, an estimate was made based on the previous works of the corresponding authors). Abbreviations: recryst., recrystallization; subl., sublimation; n.a., not available. <sup>b</sup> Reference 6. <sup>c</sup> Reference 7. <sup>d</sup> Reference 8. <sup>e</sup> Reference 9. <sup>f</sup> Reference 10.

required encapsulation procedure was applied. The sealing in polymer bags prevented sublimation of the sample before burning in the oxygen atmosphere. There were some concerns regarding addition of hydrocarbon oils for facilitation of the combustion process.<sup>7</sup> Indeed, the sample of solid adamantane could be partially dissolved in the oil. However, adamantane has a low solubility in common alkanes, and this process should be extremely slow due to the high viscosity of the oil. Nonetheless, the combustion result from ref 7 agrees well with the other values given in Table 4. Thus, we found no dependence of  $\Delta_c H_m^\circ$  values listed in Table 4 on the auxiliary compounds used.

Taking into account the good agreement of the  $\Delta_c H_m^\circ$  values for crystalline adamantane from Table 4, the average-weighted value  $\Delta_c H_m^\circ$  (cr, 298.15 K) = -6030.4 ± 1.5 kJ·mol<sup>-1</sup> was derived using all literature and our data, except that from ref 6. Its uncertainty ( $\varepsilon_{av}$ ) was calculated using the uncertainty for each  $\Delta_c H_m^\circ$  value ( $\varepsilon_i$ ) and the deviation of each value from the average-weighted one ( $x_i - \langle x \rangle$ ) by the following formula

$$\varepsilon_{av} = 1/\sqrt{\sum_i 1/\{\varepsilon_i^2 + (x_i - \langle x \rangle)^2\}} \quad (7)$$

The standard molar enthalpy of formation of adamantane in the crystalline state,  $\Delta_f H_m^\circ$  (cr, 298.15 K) = -191.4 ± 2.0 kJ·mol<sup>-1</sup>, based on the reaction



was obtained from the enthalpy balance for reaction 8 according to Hess's law by use of the molar enthalpies of formation of liquid H<sub>2</sub>O,  $\Delta_f H_m^\circ$  (H<sub>2</sub>O, liq) = (-285.83 ± 0.04) kJ·mol<sup>-1</sup>, and gaseous CO<sub>2</sub>,  $\Delta_f H_m^\circ$  (CO<sub>2</sub>, g) = (-393.51 ± 0.13) kJ·mol<sup>-1</sup> taken as recommended by CODATA.<sup>37</sup> The uncertainty assigned to  $\Delta_f H_m^\circ$  is a combined uncertainty, including the uncertainty calculated by eq 7 and the uncertainties of the enthalpies of formation of the reaction products H<sub>2</sub>O and CO<sub>2</sub>.

On the basis of the formation enthalpy for the crystalline state and the sublimation enthalpy obtained in the present work at *T* = 298.15 K, the following ideal-gas formation enthalpy was derived:  $\Delta_f H_m^\circ$  (g, 298.15 K) = -132.3 ± 2.2 kJ·mol<sup>-1</sup>. The enthalpy of formation for the ideal-gas at *T* = 298.15 K was adjusted to other temperatures by use of thermodynamic functions of the elements<sup>37,38</sup> and adamantane (Table 3).

## ■ ASSOCIATED CONTENT

**S Supporting Information.** Auxiliary quantities for the combustion calorimetry (Table S1); experimental molar heat capacities of adamantane at saturated vapor pressure (Table S2); scaling factors ( $\chi$ ) for the calculated wave numbers of the normal vibrations ( $\omega$ ) of adamantane (Table S3); results from combustion calorimetry (Tables S4 and S5). This material is available free of charge via the Internet at <http://pubs.acs.org>.

## ■ AUTHOR INFORMATION

### Corresponding Author

\*Phone: +375-17-200-3916 (G.J.K.); +49-381-498-6508 (S.P.V.). Fax: +375-17-200-3916 (G.J.K.); +49-381-498-6502 (S.P.V.). E-mail: [kabo@bsu.by](mailto:kabo@bsu.by) (G.J.K.); [sergey.verevkin@uni-rostock.de](mailto:sergey.verevkin@uni-rostock.de) (S.P.V.).

## ■ ACKNOWLEDGMENT

The research done in Rostock has been supported by the German Science Foundation (DFG) in the frame of the priority program SPP 1191 "Ionic Liquids". Products or companies are named solely for descriptive clarity and neither constitute nor imply endorsement by NIST or by the U.S. government.

## ■ REFERENCES

- (1) Pimerzin, A. A.; Sarkisova, V. S.; Roschupkina, I. Y. *Izv. Vyssh. Uchebn. Zaved. Khim. Khim. Tekhnol.* **1999**, 42 (3), 57–63.
- (2) Karpushenkava, L. S.; Kabo, G. J.; Bazyleva, A. B. *J. Mol. Struct.: THEOCHEM* **2009**, 913 (1–3), 43–49.
- (3) Chang, S.-S.; Westrum, E. F., Jr. *J. Phys. Chem.* **1960**, 64, 1547–1551.
- (4) Kabo, G. J.; Blokhin, A. V.; Charapennikau, M. B.; Kabo, A. G.; Sevruck, V. M. *Thermochim. Acta* **2000**, 345, 125–133.
- (5) Van Ekeren, P. J.; van Genderen, A. C. G.; van den Berg, G. J. K. *Thermochim. Acta* **2006**, 446, 33–35.
- (6) Månsson, M.; Rapport, N.; Westrum, E. F., Jr. *J. Am. Chem. Soc.* **1970**, 92, 7296–7299.
- (7) Butler, R. S.; Carson, A. S.; Laye, P. G.; Steele, W. V. *J. Chem. Thermodyn.* **1971**, 3, 277–280.
- (8) Boyd, R. H.; Sanwal, S. N.; Shary-Tehrany, S.; McNally, D. *J. Phys. Chem.* **1971**, 75, 1264–1271.
- (9) Clark, T.; Knox, T. Mc. O.; McKerver, M. A.; Mackle, H.; Rooney, J. J. *J. Am. Chem. Soc.* **1979**, 101, 2404–2410.
- (10) Miroshnichenko, E. A.; Lebedev, V. P.; Matyushin, Yu. N. *Dokl. Phys. Chem.* **2002**, 382 (4–6), 40–42. (translated from *Dokl. Akad. Nauk* **2002**, 382 (4), 497–499).



- (11) Van Roon, A.; Parsons, J. R.; Govers, H. A. J. *J. Chromatogr. A* **2002**, 955, 105–115.
- (12) Chickos, J. S.; Hosseini, S.; Hesse, D. G. *Thermochim. Acta* **1995**, 249, 41–62.
- (13) Reiser, J.; McGregor, E.; Jones, J.; Enick, R.; Holder, G. *Fluid Phase Equilib.* **1996**, 117, 160–167.
- (14) Chickos, J.; Hesse, D.; Hosseini, S.; Nichols, G.; Webb, P. *Thermochim. Acta* **1998**, 313, 101–110.
- (15) Mokbel, I.; Ruzicka, K.; Majer, V.; Ruzicka, V.; Ribeiro, M.; Jose, J.; Zabransky, M. *Fluid Phase Equilib.* **2000**, 169, 191–207.
- (16) Florian, W. Z. *Phys. Chem.* **1968**, 61, 319–321.
- (17) Jochems, R.; Dekker, H.; Mosselman, C.; Somsen, G. J. *Chem. Thermodyn.* **1982**, 14, 395–398.
- (18) Lee, W. Y.; Slutsky, L. J. *J. Phys. Chem.* **1975**, 79, 2602–2604.
- (19) Wu, P.-J.; Hsu, L.; Dows, D. A. *J. Chem. Phys.* **1971**, 54, 2714–2721.
- (20) Bratton, W. K.; Szilard, I.; Cupas, C. A. *J. Org. Chem.* **1967**, 32, 2019–2021.
- (21) Frenkel, M.; Chirico, R. D.; Diky, V.; Yan, X.; Dong, Q.; Muzny, C. J. *Chem. Inf. Model.* **2005**, 45, 816–838.
- (22) Diky, V.; Muzny, C. D.; Lemmon, E. W.; Chirico, R. D.; Frenkel, M. J. *Chem. Inf. Model.* **2007**, 47, 1713–1725.
- (23) Diky, V.; Chirico, R. D.; Kazakov, A. F.; Muzny, C. D.; Frenkel, M. J. *Chem. Inf. Model.* **2009**, 49, 503–517.
- (24) Frenkel, M.; Chirico, R. D.; Diky, V. V.; Muzny, C.; Kazakov, A. F.; Lemmon, E. W. *NIST ThermoData Engine, NIST Standard Reference Database 103b—Pure Compounds and Binary Mixtures, Version 3.0*; National Institute of Standards and Technology, Standard Reference Data Program: Gaithersburg, MD, 2008.
- (25) Blokhin, A. V.; Paulechka, Y. U.; Kabo, G. J. *J. Chem. Eng. Data* **2006**, 51, 1377–1388.
- (26) Bazyleva, A. B.; Blokhin, A. V.; Kabo, A. G.; Kabo, G. J.; Emel'yanenko, V. N.; Verevkin, S. P. *J. Chem. Thermodyn.* **2008**, 40, 509–522.
- (27) Coops, J.; Jessup, R. S.; Van Nes, K. In *Experimental Thermochemistry. Measurement of Heats of Reaction*; Rossini, F. D., Ed.; Interscience Publishers Inc.: New York, 1956; pp 27–58.
- (28) Emel'yanenko, V. N.; Verevkin, S. P.; Heintz, A. J. *Am. Chem. Soc.* **2007**, 129, 3930–3937.
- (29) Hubbard, W. N.; Scott, D. W.; Waddington, G. In *Experimental Thermochemistry. Measurement of Heats of Reaction*; Rossini, F. D., Ed.; Interscience Publishers Inc.: New York, 1956; pp 75–128.
- (30) Wieser, M. E.; Coplen, T. B. *Pure Appl. Chem.* **2011**, 83, 359–396.
- (31) Frenkel, M.; Kabo, G. J.; Marsh, K. N.; Roganov, G. N.; Wilhoit, R. C. *Thermodynamics of Organic Compounds in the Gas State*; TRC Data Series; Thermodynamics Research Center: College Station, TX, 1994; Vol. 1.
- (32) Granovsky, A. A. *PC GAMESS*, version 7.0; <http://classic.chem.msu.su/gran/games/index.html>
- (33) Bistričić, L.; Baranović, G.; Mlinarić-Majerski, K. *Spectrochim. Acta, Part A* **1995**, 51, 1643–1664.
- (34) Bailey, R. T. *Spectrochim. Acta Part A* **1971**, 27, 1447–1453.
- (35) Jenkins, T. E.; Lewis, J. *Spectrochim. Acta Part A* **1980**, 36, 259–264.
- (36) *NIST Computational Chemistry Comparison and Benchmark Database, NIST Standard Reference Database Number 101, Release 15a*; Johnson III, R. D., Ed.; National Institute of Standards and Technology: Gaithersburg, MD, Apr 2010; <http://cccbdb.nist.gov>.
- (37) Cox, J. D.; Wagman, D. D.; Medvedev, V. A. *CODATA Key Values for Thermodynamics*; Hemisphere Publishing Corp.: New York, 1989.
- (38) *Thermodynamic Properties of Individual Substances*, 4th ed.; Gurvich, L. V., Veyts, I. V.; Alcock, C. B., Eds.; Hemisphere Publishing Corp.: New York, 1989.